NATIONAL AERONAUTICS AND SPACE ADMINISTRATION

Technical Memorandum 33-675

Explosive Propulsion Applications

Y. Nakamura

G. Varsi

L. H. Back

JET PROPULSION LABORATORY

CALIFORNIA INSTITUTE OF TECHNOLOGY

PASADENA, CALIFORNIA

April 1, 1974

NATIONAL AERONAUTICS AND SPACE ADMINISTRATION

Technical Memorandum 33-675

Explosive Propulsion Applications

Y. Nakamura
G. Varsi
L. H. Back

JET PROPULSION LABORATORY
CALIFORNIA INSTITUTE OF TECHNOLOGY
PASADENA, CALIFORNIA

April 1, 1974

Prepared Under Contract No. NAS 7-100
National Aeronautics and Space Administration

PREFACE

The work described in this report was performed by the Propulsion Division of the Jet Propulsion Laboratory.

ACKNOWLEDGMENT

The authors thank the following individuals for providing valuable assistance during the course of this study: E. Wong, Aerojet Solid Propulsion Company; Capt. R. F. Bestgen, Air Force Institute of Technology; Capt. J. R. Nunn, AFRPL; and Dr. S. Gill, Artec Associates.

CONTENTS

TABLES

FIGURES

ABSTRACT

The feasibility and application of an explosive propulsion concept capable of supporting future unmanned missions in the post-1980 era were examined and recommendations made for advanced technology development tasks. The Venus large lander mission was selected as the first major undertaking in which the explosive propulsion concept can find application. A conceptual design was generated and its performance, weight, costs, and interaction effects with other spacecraft subsystems determined. Comparisons were made with conventional propulsion alternatives, primarily on the basis of performance and spacecraft interaction effects. The results of this study verified the feasibility of the explosive propulsion system for planetology experiments within the dense atmosphere of Venus as well as the outer planets. Additionally, it was determined that the Venus large lander mission could be augmented ballistically with significant delivery margin in which added mission capability could be exploited.

I. INTRODUCTION

A continuing interest exists in developing advanced techniques for use in future exploration of the solar system. Particular interest is evident in developing probes which can penetrate the dense atmospheres of Venus and the major planets to great depths. Propulsion capabilities for these types of missions will be taxed both in meeting the performance requirements and in operating in the high pressure and temperature environment indigenous to these target planets (e.g., Venus, Jupiter, Saturn, Uranus).

The performance of a conventional chemical propulsion system is known to decrease drastically with the decrease of the ratio of chamber pressure to ambient pressure (P_c/P_a). Typically, the specific impulse is halved when the ambient pressure reaches ~10^5 to 10^6 Pa (see Section V-A). As the ambient pressure increases further, the inadequacy and excessive penalties associated with chemical rockets become increasingly evident.

Propulsion by means of a detonating propellant appears to be particularly suited to operation in a high-pressure environment. Chemical explosive propulsion is one of a broad range of advanced concepts that was evaluated for potential application in the post-1990 time period (Ref. 1). Since this concept appeared technically promising and some possible early missions had been identified for this concept (as early as the 1980's), a separate, in-depth study was initiated to evaluate potential planetary mission applications.

II. PROGRAM OBJECTIVES AND SCOPE

The objectives of this study are (1) to investigate the potential of employing various explosive propulsion concepts for application to future unmanned missions in the post-1980 era, (2) to identify the most promising

concepts as a function of mission type for those missions of probable concern to NASA, and (3) to determine advanced technology development tasks required to bring the concepts to fruition.

The scope of this activity included the evaluation of both primary and secondary propulsion schemes to support planetology experiments. Candidate system performance capability was assessed in terms of representative mission profiles to evaluate their applicability to various propulsive modes within the demanding environments of dense atmospheric planets. Included in this analysis was a preliminary assessment of the interactions arising from the integration of the propulsive subsystem with other spacecraft subsystems.

Mission feasibility was examined under the constraints of performance, timing, and availability of supporting technologies. Conventional propulsion alternatives were then compared with the promising explosive propulsion concepts that were identified. This comparison was based primarily on performance and spacecraft interaction effects. The effects of costs and likelihood of potential public support for the mission received cursory examination.

III. CONCEPT DESCRIPTION

A. CONCEPT DEFINITION AND CHARACTERISTICS

The explosive propulsion concept entails a series of controlled sequential detonations to propel a payload to significant velocities. Explosive propulsion systems are characterized by the following unique system features:

(1) Performance increase at higher ambient pressures.

(2) Enhancement of delivered specific impulse with increasing density of the atmospheric medium.

(3) Microsecond response, precision impulse propulsive capability that can be commanded for multiple start-stop operation.

(4) Ability to tailor the total impulse and peak loads delivered to the spacecraft (i. e., selection of explosives (Refs. 2, 3, and 4),[1] explosive formulation (Refs. 5, 6, 7, and 8), firing rate, charge configuration (approaching critical diameter) of solid explosives (Refs. 9 and 10), and use of attenuators (Ref. 11)).

(5) Capability of being heat-sterilized with potentially less detrimental effects than experienced with contemporary solid-propellant rockets.

(6) Ability to perform delicate measurements without interference from the propulsion subsystem (between pulses) if the repetition rate is low.

Additionally, because of the pulsing mode of operation, the detonating pressures developed do not have to be contained statically by the structure but only dynamically during the interval of the detonation (i. e., a few microseconds). Hence, the mechanization of an operating system is not expected to be realized at the expense of excessive superstructure weight.

For the mission application selected, many of the above-mentioned innovations available for tailoring the total impulse and peak loads were discarded because of their limitations in meeting mission-peculiar requirements. For example, although intermediate rate reactions are frequently observed in condensed explosives (Ref. 3) and have been studied by numerous investigators, they are still not fully understood. In addition, they have yet to be applied in practical devices, primarily because they have not yet exhibited sufficient stability of properties. In general, the utility of any design innovation that is dependent upon the amount of energy losses in the lateral expansion process (i. e., critical diameter, ideal detonation in low-density media, unstable low-velocity detonation in very weak containers, etc.) would be suspect owing to the high pressure environment in which the explosive propulsion system must be operational.

[1] Properties of typical explosives and their performance potential are further delineated in the Appendix.

The use of porous attenuators (foams) (Ref. 11) is also questionable in view of the high back (atmospheric) pressure expected within the divergent nozzle. Homogeneous low-density attenuators, in conjunction with solid explosive charges, may be feasible but their employment will be accompanied by lower packaging efficiency, elaborate feed mechanism, and attendant weight penalty. Furthermore, since the simulation experiments on Project Orion (Ref. 12) have shown that peak pressures up to 9×10^8 Pa (9 kbars) could be successfully accommodated in steel (~50% above its elastic limit), there is little likelihood of any severe technological barriers that would prevent the mechanization of a standoff scheme (see Section V-E) or expendable stem from ultimately being developed.

B. ANALYTICAL AND DESIGN PROPOSALS

Early conceptual designs evolving from flier plate techniques employed alternating layers of solid high-explosive wafers and attenuating low-density materials (Fig. 1) in an attempt to reduce the peak shock strength and to spread the resultant pressure pulse over a longer period of time (Ref. 13). The stacked array of explosive charges and attenuators was attached to the payload through a shock-absorbing device patterned after a configuration developed for the Orion simulation experiments (Ref. 12).

Various design options were proposed in which the discrete explosive layers could be initiated sequentially but independently upon command, or by shock waves generated by the detonation of preceding charge(s) as in a conventional explosive train. Inasmuch as these designs were formulated without the use of a combustion chamber or nozzle, a significant reduction in the inert mass was postulated.

Excessive increases (as large as a factor of 2) in specific impulse (I_s) over conventional solid-propellant rockets were claimed for near-Earth applications (Ref. 13). Clearly the energy released per unit mass by a chemical explosive is of the same order (5-7 MJ $\cdot$ kg^{-1}) as available in chemical propellants. The maximum specific impulse achievable by explosives is, therefore, somewhat less than that derived from conventional propellants because the conversion of thermal energy into momentum of

resultant gases is less efficient in a detonation than in a nozzle expansion. Further, the nonuniformity of the velocity distribution of detonation gases causes a loss in specific impulse, which has been shown to be of the order of 15%.

Numerical analyses by one-dimensional hydrodynamic codes have shown that the specific impulse theoretically obtainable by a conventional explosive, such as Composition B, detonating against a steel acceptor plate is approximately 2160 to 2450 $N \cdot s \cdot kg^{-1}$ (220 to 250 $lbf \cdot s \cdot lbm^{-1}$) (Refs. 14 and 15). Typically the maximum achievable performance level from explosive propulsion devices is characterized by an I_s = 3140 $N \cdot s \cdot kg^{-1}$ (320 $lbf \cdot s \cdot lbm^{-1}$) that corresponds to the deliverable output of a high-energy aluminized explosive of the MOX-1 type (35% AP, 26% Al, 26% Mg, 10% tetryl, and 3% filler).

An examination of the associated kinetics suggests that an increase in the specific impulse of ~20% can be realized through the use of a discharge nozzle. This improvement in performance is ascribed to the beneficial effects derived from directional expulsion of the detonation gases. It was further speculated that in dense atmospheric environments the expulsion of the entrained atmospheric gases in the discharge nozzle should give rise to a significant enhancement in the performance of explosive propulsion devices.

C. EXPERIMENTAL EVOLUTION

Under related funding, a low-level experimental program was initiated at the Jet Propulsion Laboratory to test the validity of these hypotheses (Refs. 16 and 17). In these experiments a vertical sled was propelled (on a guy-wired test track) by the detonation of single- and multiple-explosive charges (Fig. 2). Experiments were run with and without a discharge nozzle in air as well as under selected conditions within a controlled environment. Although the design of the test apparatus was not expressly tailored for performance optimization (but adopted for convenience of manufacture), specific impulses of ~ 2160 $N \cdot s \cdot kg^{-1}$ (220 $lbf \cdot s \cdot lbm^{-1}$) were repeatedly obtained by detonating Detasheet explosive charges (85% PETN, 15% wax).

A compilation of significant results obtained in these experiments is presented in Table 1. It is important to note the near-linearity of resultant velocities for single-, double-, and triple-charge experiments observed with little or no degradation in specific impulse. Of greater significance, however, is the substantiation of the relative benefits of incorporating a discharge nozzle and of operating in a high back-pressure environment such as CO_2 selected on the basis of the Venusian atmospheric composition. For example, the measured increase in I_s is twofold (5680:2500 $N \cdot s \cdot kg^{-1}$) in going from 1×10^5- to 84.5×10^5- Pa (1- to 84.5-bar) atmospheric pressure. (A further exposition on performance predictions is presented in Section V-B).

In related tests, the feasibility of initiating thixotropic high-explosive charges with a pulsed laser beam has been substantiated (Ref. 16). Additional studies are currently under way to assess the mechanization of a repetitive laser initiation technique.

The concomitant theoretical effort at the Jet Propulsion Laboratory focused upon the formulation of an approximate analytical model based upon blast wave theory similitude to gain insight on the important features of explosive propulsion. In this model the detonation/interaction process is approximated by neglecting the mass of the propellant in comparison with the mass of the ambient gases present in the nozzle and applying to these gases the energy released by the explosion. Additionally, monodimensional numerical calculations are being performed with existing hydrodynamic computer codes which can describe the interaction between the products of explosion and the ambient gases. More complete two-dimensional numerical calculations have been initiated.

D. BASELINE DESIGN

A schematic of a promising mechanization design is shown in Fig. 3. In this concept, the propellant is a fluid of high viscosity (possibly thixotropic), which is extruded from the reservoir onto the plunger tip. The tip is then advanced into the nozzle to a standoff sufficient to preclude sympathetic detonation of the supply propellant. At this position, it is detonated by the impingement of a focused laser pulse. The laser beam is

delivered through the bore in the plunger shaft. A blast wave attenuator at the other end of the plunger diverts and diffuses the products of explosion flowing back through the bore so that no damage is inflicted upon the laser optics.

The impulse is delivered to both the plunger and the nozzle, with the higher acceleration being delivered to the plunger. A shock absorber elastically couples the plunger to the propulsion system structure and conditions the intensity and duration of the impulse delivered to the spacecraft. The firing cycle is repeated at a frequency consistent with the total delivered impulse desired, nozzle fill rate, and maximum permissible acceleration.

An alternative of considerable interest is the operation of the plunger at high frequency (>100 Hz) to cause the explosive charge to detach from it at the end of its excursion. The charge would then be laser-detonated while no structural part is in contact with it. This approach is very attractive when high repetition is required because the stresses on the structure would be considerably reduced. Such a gap or standoff has been shown to be very effective in eliminating erosion on structural parts, although the effects, if any, upon specific impulse are not well understood at this time.

IV. APPLICATION ANALYSIS

A. GENERAL REQUIREMENTS

The current state of the art of aerodynamic entry structures is summarized as follows: (1) Venus entry has been accomplished, and (2) airfoils (deployable in motion) are difficult to design and develop in the presence of unknown flow parameters. Therefore, one is inclined to look for other solutions.

Thus, a need exists to explore propulsion concepts for operation in the dense atmospheres of the planets. The concept to be explored herein employs detonating propellant that develops pressures of 20×10^8 - 200×10^8 Pa (20 - 200 kbars) to overcome the high external pressures and achieve an acceptable expansion ratio. Such a system would be insensitive to pressure (in the sense that its expansion ratio would be practically

infinite) and would be able to function equally well in a vacuum as well as in a dense atmosphere.

For extraterrestrial applications aerodynamic surfaces and deployable parachutes may offer adequate solutions if only a direct entry hard landing were required. There are, however, several missions where active propulsion and attitude control may be necessary to fulfill mission-peculiar propulsive and maneuvering requirements. These include:

(1) Accurate imaging capability.

(2) Sample return.

(3) Information transmission (when the absorption coefficient of the atmosphere forbids radio transmissions, a probe that can periodically "surface" and transmit the data gathered in deep penetrations can offer an advantageous alternative to a series of stacked "repeater" probes).

(4) Uncertainty in the atmospheric models postulated.

(5) Severe atmospheric turbulence (i.e., 3-25 $m \cdot s^{-1}$ (Ref. 18) and 100 $m \cdot s^{-1}$ (Ref. 19) winds on Venus and Jupiter, respectively).

In any case the aerodynamic surfaces will have to be designed to withstand and operate in:

(1) Widely varying density and pressure regimes (~5 orders of magnitude).

(2) Unknown conditions of flow dynamics.

(3) Very severe entry conditions (e.g., ablation loss on the order of 17.5% (Ref. 20) for Venus and 35% (Ref. 21) for Jupiter entry).

B. POTENTIAL MISSIONS

The Advanced Propulsion Comparison (APC) (Ref. 22) and von Braun (Ref. 23) Mission Models were selected as being representative of NASA's evolving space exploration program over the next several decades. A compilation of potential missions proposed by the von Braun, APC Base

Case, and APC Extended Models is presented in Table 2. To capitalize upon the unique features of the explosive propulsion system, potential mission applications were limited to explorations requiring propulsive maneuvers within the dense planetary atmospheres. Hence, typical propulsive applications to be considered reduce to steering propulsion for atmospheric entry probes, attitude stabilization propulsion, cruise (maneuver) propulsion for a buoyant station, retro propulsion, and ascent propulsion for landing and sample return missions.

Although there are several proposed missions in which entry probes are expected to play a predominant role in planetary exploration, it is anticipated that the necessary descent maneuvers and attitude control for these devices will be effected through the deployment of suitable parachutes. Within the planning horizon encompassed by the mission models, the first major undertaking in which explosive propulsion may find application is the 1989 Venus large lander. For this mission a need is recognized for a large aeroshell, several staged parachutes, possible descent propulsion, and descent attitude control to survive and/or accomplish the severe entry pulse, descent maneuver, and final touchdown.

The remaining segments of the study accordingly focused upon an application analysis of a soft lander in the Venusian environment.

C. SCIENTIFIC OBJECTIVES AND INCENTIVES

By the time of the Venus large lander undertaking, precursor investigations will have been accomplished by Pioneer probes (atmospheric measurements), Pioneer orbiter (mapping of the fields and particle interactions), and the Venus radar mapper (mapping of surface and candidate landing sites to 100-m and 10-m resolutions, respectively). In addition, the Russian landing missions will have provided information concerning bulk density, hardness, and shallow stratification, if any, of the surface material.

The scientific objectives of the large lander are then to extend our basic understanding of the phenomenology of the physical origin and

evolution of the solar system and its workings at the present time through the acquisition of the following critical information:

(1) Definitive measurements of the chemical and isotopic composition, petrographic nature of the surface material, and local topography in scales from centimeters to meters.

(2) Measurements of the planet radius at the landing site, albedo and phase dependence of visible light, surface temperature, seismic activity, and surface radioactivity.

(3) Measurements of the local atmospheric composition, temperature, pressure, winds, and atmospheric scatterers for correlation with earlier atmospheric probes.

The ability of delicate instruments to function after soft impact makes the soft lander particularly valuable for obtaining precision measurements on the surface of the target planet. Moreover, if the lander is long lived, it provides an added dimension of detecting many time-dependent phenomena.

In general, there are a number of scientific and engineering incentives for the early concentration upon planetary exploration of Venus. These include less demanding requirements on launch velocity, spacecraft system, and telecommunications because of the closeness to Earth. Additionally, existing solar cell power sources are adequate, thermal control is easier, and atmospheric entry requirements are less taxing than for the outer planets. Further, the closer distance should provide the acquisition of a superior state of knowledge through ground-based optical, radio, and radar observations and the design of future experiments with greater confidence (Ref. 24).

D. MISSION AND SPACECRAFT REQUIREMENTS

For purposes of this study, the findings of the Advanced Propulsion Comparison (APC) Study (Ref. 22) were assumed to be a suitable data base upon which to build in determining mission, payload, and launch vehicle

performance requirements. Pertinent developments and recommendations arising from the conduct of this study are summarized as follows:

(1) Although complementary data could be provided by the addition of an orbiter, a direct entry baseline mission was assumed for the Venus large lander. Based on existing radar mapping data, two different major geological provinces would be selected for the landing sites. Sunny-side descent is desirable but not mandatory. Required surface lifetime is a minimum of 48 hours.

(2) Estimated payload weight and power requirements appropriate for the Venus lander mission are presented in Table 3. A non-propulsive lander mass of 584 kg was also allocated (Table 4) to embody growth features beyond the Viking lander that includes added entry, descent, and surface survival capabilities. It was further assumed that inheritance from other programs would be low and that considerable redundancy would be required to ensure achieving a high probability of mission success.

Entry sequence and requirements assumed for this mission are as follows. A suitable aeroshell would be incorporated to survive the high-speed deceleration environmental loads at entry. Accelerometer and timing signals would then activate the parachute activation sequence. The drogue chute is deployed at a preselected entry velocity (e.g., Mach 1.5) to stabilize the lander prior to main chute extraction. At an acceptable reduced speed (e.g., Mach 0.7), the main chute is deployed and upon full inflation the remnants of the aeroshell and heat shield are jettisoned. After main chute ejection, the lander continues the final descent and touchdown maneuvers. To accommodate the uncertainties in the atmospheric model and to provide flexibility in the descent trajectory, a final descent maneuver ΔV requirement of 500 $m \cdot s^{-1}$ was established.

Major problem areas envisioned include survival for surface operation at extreme temperatures (~700 K), touchdown maneuver in high back pressure environment (~90×10^5 Pa (~90 bars)), and sampling of both the surface and atmosphere at these elevated ambient temperatures and

pressures. Telecommunication signal attenuation and fluctuations from atmospheric turbulence may prove to be a problem if X-band frequencies were to be employed. In particular, fluctuations in the doppler signals may create tracking problems and cause loss of Earth lock. However, these problem areas are expected to be alleviated significantly through the use of S-band frequencies (Ref. 25).

V. CONCEPTUAL DESIGN EVALUATION

A. LIMITATIONS OF CONVENTIONAL CHEMICAL PROPULSION

To provide a basis for evaluating the performance of an explosive propulsion system, the following relation for specific impulse was assessed for steady-state isentropic flow in a chemical propulsion system:

$$I_s = \lambda \frac{u_e}{g_c} + \frac{(P_e - P_a) A_e}{\dot{m}} \tag{1}$$

where

I_s = specific impulse

λ = $(1 + \cos \theta)/2$ = divergence factor for a conical nozzle with divergent half-angle θ

u_e = exit velocity

g_c = conversion constant

P_e = gas pressure at exit plane

P_a = ambient pressure

A_e = nozzle cross-sectional area at exit plane

$\dot{m}$ = mass flow rate

The exit velocity is given by

$$u_e = \left\{ \frac{2\gamma}{\gamma - 1} RT_t \left[1 - \left(\frac{P_e}{P_t} \right)^{(\gamma-1)/\gamma} \right] \right\}^{1/2} \tag{2}$$

where

γ = specific heat ratio

R = gas constant

T_t = stagnation condition temperature

P_t = stagnation condition pressure

and the mass flow rate for choked flow is

$$\dot{m} = C_D P_t A_{th} \left[\frac{\gamma}{RT_t} \left(\frac{2}{\gamma + 1} \right)^{(\gamma+1)/(\gamma-1)} \right]^{1/2} = \frac{C_D f(\gamma) P_t A_{th}}{(RT_t)^{1/2}} \tag{3}$$

where

C_D = flow coefficient

A_{th} = nozzle throat cross-sectional area

Introducing ΔP as the difference between the stagnation pressure P_t in the nozzle and the ambient pressure P_a, i.e.,

$$\Delta P = P_t - P_a \tag{4}$$

then the specific impulse can be written as follows to indicate the explicit dependence on the parameters involved:

$$I_s = \frac{\lambda u_e}{g_c} + \left(\frac{P_e}{P_t} - \frac{P_a}{\Delta P + P_a} \right) \frac{(RT_t)^{1/2}}{C_D f(\gamma)} \epsilon \tag{5}$$

where ϵ is the expansion area ratio. For a given gas at a stagnation temperature T_t, flow coefficient C_D, and divergence factor λ, the specific impulse depends upon the expansion area ratio ϵ of the nozzle and the ambient pressure for a specified value of ΔP since both the exit velocity and the exit pressure ratio P_e/P_t depend only upon ϵ.

Values obtained from Eq. (5) are shown in Fig. 4. Here the specific impulse obtained from anhydrous hydrazine (80% ammonia dissociated molecular weight of 11.7 g/g • mol and $\gamma = 1.32$) is computed as a function of ambient pressure P_a, for a combustion temperature of 1000 K, nozzle flow coefficient C_D of 0.95, and a divergence factor λ of unity for nozzles with expansion area ratios ϵ of 1, 10, and 100. The combustion or stagnation pressure is not kept constant but instead is increased as the ambient pressure increases so that the pressure differential ΔP across the chamber wall remains constant. This constraint is imposed to limit the maximum stress that the materials used must withstand at a given chamber temperature.

The calculations were terminated at an ambient pressure $P_{a_{max}}$ using the Summerfield criterion so that shock-induced flow separation would not occur in the nozzle:

$$P_e \simeq 0.4\, P_{a_{max}} \tag{6}$$

From Eqs. (4) and (6) and the functional relationship $P_e/P_t\,(\gamma, \epsilon)$, the following dependence of $P_{a_{max}}$ on ΔP and ϵ is obtained:

$$P_{a_{max}} = \frac{\Delta P}{\left[\frac{0.4}{(P_e/P_t)} - 1\right]} \tag{7}$$

For the sonic nozzle ($\epsilon = 1$), calculations were also made for unchoked flow by using the appropriate mass flow rate.

The performance curves presented in Fig. 4 indicate the penalty imposed for operation at higher ambient pressures where nozzles with smaller expansion area ratios would be required to extend the operating range. The crosses denote the maximum ambient pressure before shock-induced flow separation would occur in the nozzle, and thus limit the utilization of larger expansion area ratio nozzles which have a better performance.

For perspective, the ranges of ambient pressures of interest in the exploration of planets are shown in Table 5.

B. EXPLOSIVE PROPULSION PERFORMANCE PREDICTION

As previously noted, the improvement in specific impulse with increasing ambient pressure has been borne out by analysis and experiments. Further, both analysis and experiments show a favorable dependence of performance on the density of the ambient gases. This effect is fundamentally understood in terms of expelling from the nozzle a mass of gas which is greater with greater density. Since this mass is not carried onboard the spacecraft (and therefore is not accountable as propellant), its effect is beneficial and yields an increase of performance approximately proportional to the square root of the density of ambient gases.

Empirical data substantiating these hypotheses in a CO_2 and N_2 atmosphere are presented in Fig. 5. In a typical planetary atmosphere the increase of temperature with depth offsets, to an extent, the increase in pressure so that the density and performance increases are reduced. A further reduction is indicated by the theory because of a temperature effect independent of the density effect previously noted.

The theoretical performance prediction postulated within the Venusian atmosphere is presented in Table 6 in terms of I_s and the relative mass of ambient gas in the nozzle ($\sigma = m_a/m_e$) for a range of altitudes varying from 35 km to the surface of the planet. For this range of conditions the primary atmospheric constituent, carbon dioxide, can be considered to be a perfect gas with $\gamma = 1.3$. The calculations were carried out for the 1.5-g Detasheet and for the 0.175-rad (10-deg) 15.2-cm nozzle.

Increases in the value of σ correspond to the spacecraft approaching the Venus surface. The specific impulse of about 1960 $N \cdot s \cdot kg^{-1}$ (200 lbf · s/lbm) is approximately constant as the surface is approached, and this primarily occurs because of the increasing ambient temperature and the importance of rarefaction effects which reduce the specific impulse. The performance, however, would exceed that for a chemical propulsion system as can be observed by comparison with Fig. 4).

Small increases in performance can be expected by selecting higher energy propellants. For example, although performance numbers presented throughout are based upon the employment of a commercially

available explosive consisting of 85% pentaerythritol tetranitrate (PETN) capable of delivering ~5.8 MJ/kg (1.39 kcal/g), the use of MOX-type explosives would yield outputs approaching 8 MJ/kg (2.0 kcal/g).

The explosive propulsion performance may be further improved if rarefaction effects were partially eliminated by allowing the nozzle to refill by drawing in ambient gas through slots in the sidewall (porous nozzle) (Ref. 17). However, since the viability of such a nozzle concept has yet to be addressed, for purposes of this evaluation an I_s of 1960 N · s/kg (200 lbf · s/lbm) has been assumed as being representative. Finally, it is important to note that if the motor is used in a retro-fire operation, then the density of gases in the nozzle would be much greater than ambient conditions due to stagnation pressure buildup.

If the likely improvements in specific impulse are realized, the comparative advantage for the explosive propulsion concept should prove even more favorable. The extent of this advantage is graphically illustrated in Figs. 6 and 7. Each of these figures[2] is normalized for a given ratio of explosive propulsion-to-conventional chemical rocket specific impulses (I_E/I_C) with the propellant mass fractions of the conventional (μ_C) and explosive propulsion (μ_E) as variables. Each of the figures is further developed for three different propulsive payload fractions, α = 0.2, 0.5, and 0.8.

C. PROPULSION SYSTEM DESIGN CHARACTERISTICS

For the Venus large lander mission selected, the baseline configuration consists of a five-nozzle propulsion system (Fig. 8) that is housed within a zero spring-rate mechanism network (Ref. 27). During boost and early phases of entry the network is locked out to provide the necessary spacecraft/lander dynamic stability. Once freed, the network provides a carriage of flexible supports yielding very low stiffness for small excursions from a pre-established datum. The desired structural transfer function

[2] The utility of these plots to determine the crossover points at which the performance or weight characteristics of one system offsets the properties of the other will be illustrated in the following section.

between propulsion system and parent spacecraft is achieved by suspending each of the nozzles independently on springs soft enough to provide the necessary rigid body frequency. In addition, each of the nozzles is guided in a telescoping plunger stem to ensure proper alignment of the nozzles throughout their stroke and to provide the necessary axial freedom to accommodate the one-minus-cosine deflection associated with the carriage translational stroke.

To minimize the effects of the dynamic coupling between spacecraft and propulsion system, a rigid body frequency $<<20$ Hz will be required. It was also assumed that the mean deflection of the translational springs would be 1000/km with only small variations.

The propulsive system necessary to negotiate the 500-m $\cdot$ s^{-1} descent maneuver was sized and the attendant weight estimated. The results of this computation are presented in Table 7 assuming an I_s = 1961 N $\cdot$ s $\cdot$ kg^{-1} (200 lbf $\cdot$ s/lbm) and a nonpropulsive lander mass ($M_{L_{NP}}$) = 583.9 kg (1284.6 lbm). The corresponding total injection package weight estimated is given in Table 8 along with the breakdown of subsystems.

Launch vehicle performance predictions generated indicated that the Venus large lander mission could be readily accomplished ballistically employing a Shuttle/Centaur launch vehicle (Table 9). As shown in the table, there is significant delivery margin (~factor of 3) for mission growth.

Impulse reaction time, average spacecraft acceleration, and total number of pulses per nozzle for representative values of charge size and average total thrust were computed and are compiled in Table 10. The firing rate assumed for each nozzle was 20 s^{-1} to permit a reasonable interval for refilling the nozzles with atmospheric gases. Explosive charge sizes in the range of 2 to 15 g were also selected as being representative of quantities that could be readily manipulated and reliably initiated.

To reduce the peak acceleration loads to reasonable levels, long impulse reaction times are desirable. However, a lower limit is usually determined by the critical diameter or geometry of the explosives, which in turn defines an equivalent mass in which the detonation reaction can be

sustained. For purposes of this study, a 2-g explosive charge with an average thrust of 400 N was selected as the lower limit and design point for the baseline system. The corresponding operational characteristics are an impulse reaction time of 105 μs, average spacecraft acceleration of $0.30\ m \cdot s^{-1}$, and 19,300 pulses per unit firing requirement (Table 10).

Assuming a 5-Hz rigid body frequency for the nozzle assemblies, a nominal deflection of ±0.05 m (1.97 in.) is predicted about the zero datum. For the selected spring rate of $24,500\ N \cdot m^{-1}$ (140 lbf/in.), the dynamic loading on each nozzle is 1230 N (276 lbf) (~2 times the static deflection loading), which is well within the design margin established for the nozzle wall.

As previously noted, parametric data were generated (Figs. 7 and 8) to assist in the comparative assessment of the explosive propulsion concept and competing conventional systems. The following example is presented to illustrate the utility of these data and the basis for pursuing the explosive propulsion conceptual design. From the entries of Tables 7 and 8, the values of $\mu_E = 0.75$ and $\alpha = 0.8$ are derived. Assuming a conservative estimate of $I_E/I_C = 2.0$, the chemical system must yield a $\mu_C > 1$ to be competitive (Fig. 7); clearly an impossibility. Even if it were assumed that the total contingency estimated (94.7 kg) were to be allocated to the explosive propulsion system inert (and, hence, $\mu_E = 0.56$), this competitive edge would not appreciably change. Secondly, for chemical propulsion systems to be operational down to the surface of Venus ($P_a \cong 10^7$ Pa (100 bars)), a sonic nozzle ($\epsilon = 1$) with excessive pressure differential across the chamber wall will be required. This constraint is necessarily imposed to circumvent deleterious interaction effects arising from asymmetric forces developed as a result of shock-induced flow separation in the nozzles. The penalties associated with this constraint are severe owing to the exclusion of higher expansion ratio, higher performance nozzles which further amplifies upon the performance supremacy of the explosive propulsion system. Therefore, on the basis of performance and interaction considerations, it was hypothesized that the conventional chemical propulsion system would not compete with the explosive propulsion system for the Venus large lander mission.

D. INTERACTION WITH SPACECRAFT SUBSYSTEMS

By designing the lander vehicle with the proper structural transfer function, no major barriers to the integration of the explosive system will remain. Although the nozzles are locally subjected to high g loadings, the parent lander components will be free of any extreme environment because of the provision for damping and isolation that will limit the dynamic loads to a value less than or equal to the vehicle static loading requirements.

In addition, the interactions between major elements of the lander, such as science, data management, etc., should be greatly alleviated as a result of the following considerations.

(1) The exploration of the Venusian atmosphere is expected to present no severe contamination problems owing to the strength of the prevailing winds.

(2) Heat sterilization of the explosives (if required) is expected to be performed with less detrimental effects than experienced with contemporary solid-propellant motors.

(3) Surface alteration at the landing site is of minor concern since the experiments are not intended to detect the presence of life.

(4) Both the baseline and enhanced science package heretofore described are limited to surface experiments. At this writing the necessity for descent measurements was undetermined. However, should descent measurements be required, no problems more complex than those derived from the employment of conventional chemical propulsion systems are anticipated.

(5) The use of S-band frequencies is expected to circumvent any major telecommunications problem areas.

(6) Other primary problem areas are not expected to be propulsion system dependent.

By comparison, both the conventional chemical and explosive propulsion systems are not expected to encounter any interaction obstacles as a result of their use. The principal drawback to the employment of a conventional chemical propulsion system is, however, the lack of performance.

E. ADVANCED DEVELOPMENT REQUIREMENTS

In order to bring the proposed mechanization scheme to a state of flight readiness in a time frame coincident with the proposed mission, the following critical areas of development must be addressed:

(1) Special nozzle design to eliminate or reduce rarefaction effects.

(2) Propellant formulation to obtain a high-energy, relatively low detonation velocity explosive that can be initiated by means of a laser pulse.

(3) Space-rated laser that is lightweight but sturdy to deliver ignition energy.

(4) Muffler design to preclude or minimize the debris that can reach the laser optics.

(5) Structural design of plunger and nozzle to reduce deformation and erosion for repeated firings up to 20,000 cycles.

The on-going research for item (1) has already been discussed. Similar studies (Ref. 28) have resulted in the experimental demonstration of an explosive formulation (80% KDNBF (potassium 4, 6-dinitro-benzo-furoxane) 20% FEFO (Bis (2, 2 dinitro-2-fluoro-ethyl) formal)) that is both fluid- and laser-ignitable. However, additional studies are required to obtain a propellant with the required properties of viscosity, adhesion, energy output, and sensitivity. For item (3), a compact laser is available that weighs ~5 kg, capable of delivering 16 J in 1-ms pulses at the rate of 0.1 pulses per second. Again, although feasibility demonstration has been accomplished, additional development is required to increase the pulse repetition rate to several pulses per second.

An effective muffler design (item 4) has been successfully tested at JPL. The design consists of a dozen discs of 2.54-cm (1.0 in.) diameter with a 0.62-cm (0.25 in.) bore, offset in such a way that the locus of bore hole centers is a helix of 0.31-cm (0.13 in.) diameter and 2.54-cm (1.0 in.) pitch. Throughout the experiments, the laser window was placed at 30.5 cm (1.0 ft) from the muffler face.

Of the critical development items delineated, the plunger design shown schematically in Fig. 3 has received the least amount of development attention. In repeated tests, the unit functioned properly without deforming. Pronounced erosion was, however, noted. Further development is required to increase the number of permissible firings to 10^4 - 10^5.

The laser is a relatively inefficient component in any energy delivery scheme. Hence, for a typical propellant charge of 5 g generating 30 kJ of propulsive energy, ~0.5 to 1 kV to the laser system (~1.5-3% of the propulsive output) is anticipated. Other initiation schemes have been considered (e.g., hypergolic compositions that would not need an external trigger) but were excluded from consideration because of their limited level of development.

A preliminary assessment for the nonrecurring and recurring costs associated with the development and delivery of flight hardware is presented in Table 11. It should be noted that the costs listed are based on 1973 dollars with production lots of 3 to 5 motors.

F. GROWTH OPTIONS

As previously noted a significant payload delivery margin exists (~factor of 3) when augmenting the Venus large lander mission ballistically employing a Shuttle/Centaur launch vehicle. Potential growth options include the addition of an orbiter to complement the surface experiments and to alleviate the telemetry communications should signal attenuation from atmospheric turbulence present a problem.

The explosive propulsion concept may also find application to the exploration of the dense atmospheres of the outer planets. Although recent JPL experiments conducted within a helium atmosphere have indicated a decrease of specific impulse with increasing P_a, the extent of this decrement was not significant (i.e., ~10% going from 1×10^5 to 50×10^5 Pa (1 to 50 bars) atmospheric pressure) by comparison with the anticipated decrease in performance of conventional chemical propulsion systems. Assuming this trend prevails, a large performance advantage may be extended to a variety of propulsive maneuvers within the major planet atmospheres for probes, buoyant stations, soft landers, and sample return missions.

VI. CONCLUSIONS AND RECOMMENDATIONS

The following conclusions and recommendations were derived as a result of this study:

(1) A representative unmanned mission (Venus large lander) in which the explosive propulsion concept will find application in the post-1980 era has been identified. The need for the explosive propulsion system arises as a result of significant decreases in the performance of conventional chemical propulsion systems when operating in a high back-pressure environment.

(2) A conceptual design of an explosive propulsion system has been formulated in support of this mission which offers no apparent technological or interaction barriers that would hamper the mechanization of this concept.

(3) The Venus large lander mission can be augmented ballistically utilizing a Shuttle/Centaur launch vehicle with a significant delivery margin by which to exploit extended mission capabilities. Recommended manipulations include the addition of a complementing orbiter.

(4) The explosive propulsion concept offers the potential of equal application to similar mission types for the exploration of the dense atmospheres of the outer planets. An examination of methods to exploit the unique features of the explosive propulsion system is recommended once the mission requirements are formulated.

REFERENCES

1. Nakamura, Y., Propulsion Concepts for Advanced Systems, Interim Progress Report, NASA No. 113-31-11-08-00, Jet Propulsion Laboratory, Pasadena, Calif., Sept. 8, 1972, (JPL internal document).

2. Wooten, D. C., Bredfeldt, H. R., Woolfolk, R. W., and Kier, R. J., Investigation of Low-Velocity Detonation Phenomenon in Liquid Propellants, Fuels and Explosives, AFOSR 70-1005 TR, Stanford Research Institute, Menlo Park, Calif., Mar. 30, 1970.

3. Brown, J. A., and Collins, M., Explosion Phenomena Intermediate Between Deflagration and Detonation, AD 662-778, Esso Research and Engineering Company, Linden, N. J., Oct. 1967.

4. Campbell, A. W., Davis, W. C., and Travis, J. R., "Shock Initiation of Detonation in Liquid Explosives," Physics of Fluids, Vol. 4, p. 498, 1961.

5. Seay, G. E., and Seely, L. B., "Initiation of a Low-Density PETN Pressing by a Plane Shock Wave," Journal of Applied Physics, Vol. 32, p. 1092, 1961.

6. Abegg, M. T., Fisher, H. J., Lawton, H. C., and Weatherill, W. T., "Low Detonation Pressure Explosives," Symposium on Explosives and Hazards and Testing of Explosives, 145th National Meeting, American Chemical Society, New York, 1963.

7. Abegg, M. T., Frombarger, J. W., Hoppeach, C. W., Meikle, W. J., and Ritenhouse, C. J., "Explosive Evaluation of Coordinate Compounds," 145th National Meeting, American Chemical Society, New York 1963.

8. D. Thatcher and R. J. Richards, Teledyne McCormick Selph, Hollister, Calif., Oct. 1972 (private communication on LVD Explosives).

9. Cook, M. A., The Science of High Explosives, Reinhold Publishing Corporation, New York, 1958.

10. Anderson, W. H., and Pesante, R. E., Eighth Symposium Combustion, Williams and Wilkins Company, Baltimore, p. 705, 1962.

11. Knapp, R. L., Precise Impulse Propulsion (PIP) Program, Report RK-73-4, Aerojet Solid Propulsion Company, Sacramento, Calif., Sept. 24, 1973.

12. Nuclear Pulsed Propulsion Project (Project Orion), Technical Summary Report (U), RTD-TDR-63-3006, Vol. IV, General Dynamics Corporation, General Atomics Division, San Diego, Calif., 1963-1964 (SRD).

13. Beichel, R. and O'Brien, C. J., Explosive Propulsion Status Report, ALRC Report ASG-7001, Aerojet General Corporation, Sacramento, Calif., Mar. 1970.

14. Gross, M., Explosive Impulse Calculations, PIFR 259, Physics International, Co., San Leandro, Calif., Nov. 1970.

15. Bestgen, R. F., and Nunn, J. R., "Propulsion Performance of Condensed-Explosive Rockets," AIAA Paper 72-1161, AIAA/SAE 8th Joint Propulsion Specialist Conference, New Orleans, La., Nov. 29 - Dec. 1, 1972.

16. Varsi, G., Back, L. H., and Dowler, W. L., "Development of Propulsion for High-Atmospheric Pressure or Dense Environments," JPL Quarterly Technical Report, Vol. 3, No. 2, pp. 45-52, Jet Propulsion Laboratory, Pasadena, Calif., July 1973.

17. Varsi, G., and Back, L. H., "Detonation Propulsion For High Pressure Environments," AIAA Paper No. 73-1237, AIAA/SAE 9th Propulsion Conference, Las Vegas, Nev., Nov. 5-7, 1973, to be published in AIAA J.

18. "Models of Venus Atmosphere (1972)," NASA Space Vehicle Design Criteria (Environment), NASA SP-8011, National Aeronautics and Space Administration, Goddard Space Flight Center, Greenbelt, Md., Sept. 1972.

19. "The Planet Jupiter (1970)," NASA Space Vehicle Design Criteria (Environment), NASA SP-8069, National Aeronautics and Space Administration, Goddard Space Flight Center, Greenbelt, Md., Dec. 1971.

20. Levine, P., Planetary Explorer Universal Bus Study, AVSD-0503-70-RR, AVCO Government Products Group, AVCO Systems Division, Wilmington, Mass., Oct. 1970.

21. Wiltshire, R. S., "Outer Planet Entry Probe Systems Study," Vol. I, Martin Marietta Corporation, Denver, Colo., Aug. 1972.

22. Briefing to the Advanced Propulsion Comparison (APC) Steering Committee, Report No. 701-138, Jet Propulsion Laboratory, Pasadena, Calif., Mar. 1, 1972 (JPL internal document).

23. von Braun, W., Updated NASA Mission Model, Office of the Administrator Memorandum, National Aeronautics and Space Administration, Washington, D. C., June 1, 1972.

24. Investigation of the Outer Solar System, The Science Advisory Group, April 1971-June 1972.

25. Woo, R., Kendall, W., Ishimaru, A., and Berwin, R., Effects of Turbulence in the Atmosphere of Venus on Pioneer Venus Radio - Phase I, Technical Memorandum 33-644, Jet Propulsion Laboratory, Pasadena, Calif., June 30, 1973.

26. "The Planet Saturn (1970)," NASA Space Vehicle Design Criteria (Environment), NASA SP-8091, National Aeronautics and Space Administration, Goddard Space Flight Center, Greenbelt, Md., June 1972.

27. Gayman, W. H., Trubert, M. R., and Abbott, P. W., Measurement of Structural Transfer Functions Significant to Flight Stability of the Surveyor Spacecraft, Technical Memorandum 33-389, Jet Propulsion Laboratory, Pasadena, Calif., May 1, 1969.

28. Menichelli, V. J., Sensitivity Data Obtained on a Variety of Explosive Mixtures Intended for Laser Initiation, IOM ED-381-73-128, Jet Propulsion Laboratory, Pasadena, Calif., July 19, 1973 (JPL internal document).

29. Engineering Design Handbook, Explosives Series, Properties of Explosives of Military Interest, AMCP 706-177, Headquarters, U. S. Army Material Command, Washington, D. C., Mar. 1967.

Table 1. Summary of explosive propulsion experimental results

Type of test	Sled mass, g	Nozzle half angle, rad (deg)	Nozzle length, cm (in.)	Environment	Atmospheric temperature, K	Atmospheric pressure, Pa × 10^5 (psia)	Sled velocity, $m \cdot s^{-1}$ ($ft \cdot s^{-1}$)	I_s, $N \cdot s \cdot kg^{-1}$ ($lbf \cdot s \cdot lbm^{-1}$)
Single pulse (no nozzle)	1197	---	---	Air	293	1.01 (14.7)	1.90 (6.24)	1490 (152)
Double pulse (no nozzle)	1197	---	---	Air	293	1.01 (14.7)	3.96 (13.0)	1550 (158)
Triple pulse (no nozzle)	1197	---	---	Air	293	1.01 (14.7)	5.64 (18.5)	1470 (150)
Single pulse (with nozzle)	1197	0.175 (10)	15.2 (6)	Air	293	1.01 (14.7)	2.74 (9.00)	2150 (219)
Dry microballoons in nozzle	1197	0.175 (10)	15.2 (6)	Air	293	1.01 (14.7)	3.93 (12.9)	6030 (615)
Water-filled nozzle (300 cm^3)	5985	0.175 (10)	15.2 (6)	Air	293	1.01 (14.7)	2.71 (8.89)	20700 (2115)
Dry nitrogen environment	2400	0.175 (10)	15.2 (6)	GN_2	293	$4 \cdot 10^{-3}$ (0.058)	1.48 (4.84)	2310 (236)
Dry nitrogen environment	2400	0.175 (10)	15.2 (6)	GN_2	293	8.27 (120)	1.69 (5.55)	2650 (270)
Dry nitrogen environment	2400	0.175 (10)	15.2 (6)	GN_2	293	68.9 (1000)	1.82 (5.96)	2840 (290)
Dry nitrogen environment	2400	0.175 (10)	3.81 (1.5)	GN_2	293	$4 \cdot 10^{-3}$ (0.116)	1.39 (4.56)	2180 (222)
Dry nitrogen environment	2400	0.175 (10)	3.81 (1.5)	GN_2	293	1.01 (14.7)	1.49 (4.88)	2320 (237)
Dry nitrogen environment	2400	0.175 (10)	3.81 (1.5)	GN_2	293	8.27 (120)	1.63 (5.34)	2550 (260)
Dry nitrogen environment	2400	0.175 (10)	3.81 (1.5)	GN_2	293	68.9 (1000)	1.76 (5.79)	2770 (282)
Dry CO_2 environment	2400	0.175 (10)	15.2 (6)	CO_2	308	1.01 (14.7)	1.60 (5.24)	2500 (255)
Dry CO_2 environment	2400	0.175 (10)	15.2 (6)	CO_2	308	25.3 (367)	1.92 (6.31)	3010 (307)
Dry CO_2 environment	4500	0.175 (10)	15.2 (6)	CO_2	308	47.2 (685)	1.13 (3.70)	3310 (338)
Dry CO_2 environment	4500	0.175 (10)	15.2 (6)	CO_2	308	69.6 (1010)	1.26 (4.14)	3710 (378)
Dry CO_2 environment	4500	0.175 (10)	15.2 (6)	CO_2	308	84.5 (1225)	1.93 (6.34)	5680 (579)

Table 2. Mission models

Mission	von Braun Model (Ref. 23)	APC Base Case Model (Ref. 22)	APC Extended Model (Ref. 22)
Encke Rendezvous	1984	1981-1982	1981-1982
Venus Radar Mapper	1984	1983	1983
Mars Semi-Autonomous Rover	1986	1984	1984
Mercury Orbiter	1987	1984	1984
Saturn Orbiter/Probe	1984	1984	1984
Asteroid Rendezvous	1989	1985	1985
Halley Flyby	Not included	1985	1985
Jupiter Orbiter	1986-1987	1985	1985
U/N (Uranus Probe)	1986	1986	1986
Uranus Orbiter (w/Probe)	*	1987	1987
Venus Large Lander	1989	1989	1989
Neptune Orbiter/Probe	*	1989	1989
Jupiter/Pluto Flyby	*	1990	1990
Satellite Orbiter/Lander	*	1990	1990
Mars Surface Sample Return	*	1990	1990
Halley Rendezvous	Not included		1983
S/U/N (Uranus Probe)	Not included		1984
0.1 - AU Solar Probe	*		1985
Saturn Ring Probe	*		1988
Asteroid Sample Return	*		1993
Phobos/Deimos Sample Return	*		1994

*The von Braun Model does not identify missions beyond 1990. Missions noted by asterisk are not necessarily excluded but would be performed after 1990.

Table 3. Typical science package for Venus large lander mission

Instrument	Mass, kg	Power, W
Baseline Science:		
TV, two cameras with periscope	20	15 (each)
Strobe light	5	5
Scanning laser range finder	5	5
Sampling arm, crusher, and siever	9	30
Mass spectrometer	6	16
Pulsed neutron/gamma spectrometer	7	30
Seismometer	5	4
Seismic sources	7	10
Surface thermal probe	2	2
Meteorology instruments	2	7
Atmospheric nephelometer	2	5
Baseline subtotal	70	
Enhanced Science:		
Petrographic microscope	6	10
X-ray spectrometer	3	5
X-ray diffractometer	4	10
Total	83	

Table 4. Nonpropulsive lander mass estimate

Subsystem	Mass, kg (lbm)
Structure	100.7 (221.5)
Pyro	11.4 (25.1)
Thermal control	90.9 (200.0)
Power	83.8 (184.4)
Telemetry	18.8 (41.4)
Guidance and control	58.8 (129.4)
Communications	29.1 (64.0)
Wire harness	25.7 (56.5)
Science	70.0 (154.0)
Contingency	94.7 (208.3)
Total estimated nonpropulsive mass	583.9 (1284.6)

Table 5. Nominal atmospheric pressure ranges of typical target planets

Altitude, km	Venus,[a] Pa $\times 10^5$ (bars)	Jupiter,[b,c] Pa $\times 10^5$ (bars)	Saturn,[c,d] Pa $\times 10^5$ (bars)
50	1	8×10^{-2}	3×10^{-1}
0[e]	95	1	1
-170	--	30	10

[a] Reference 18.

[b] Reference 19.

[c] For purposes of evaluating growth applications, the comparative characteristics and performance predictions in the atmospheres of representative Jovian planets were also developed.

[d] Reference 26.

[e] Altitude of zero is arbitrarily set at a pressure of one Earth atmosphere.

Table 6. Venus propulsive performance prediction

Elevation, km	T_a, K	P_a, Pa × 10^5 (bars)	ρ_a,* g · cm^{-3} × 10^2	σ	I_s	
					N · s · kg^{-1}	(lbf · s/lbm)
0	750	95.2	6.57	14.0	1820	(186)
5	710	69.6	5.11	10.8	1760	(179)
10	670	49.9	3.90	8.21	1840	(188)
15	629	35.1	2.93	6.15	1930	(197)
20	587	24.0	2.15	4.50	2000	(204)
25	545	16.0	1.55	3.23	2060	(210)
30	502	10.3	1.09	2.25	2030	(207)
35	457	6.4	0.74	1.55	1940	(198)

* ρ_a = Density of atmospheric gases.

Table 7. Propulsion subsystem mass estimate[a]

Component	Mass, kg (lbm)
Structure/adapters	10.2 (22.4)
Reservoir and delivery system	13.9 (30.6)
Lasers and optics	13.0 (28.6)
Plungers and shock absorbers	20.0 (44.0)
Mufflers	2.5 (5.5)
Nozzles	12.5 (27.5)
Inert weight	72.1(158.6)
Explosives	216.3(475.9)
Total propulsion subsystem	288.4(634.5)

[a] $\Delta V = 500\ m \cdot s^{-1}$; $I_s = 1961\ N \cdot s \cdot kg^{-1}$ (200 lbf • s/lbm); $M_L = 583.9$ kg (1284.6 lbm).

Table 8. Estimated injection package mass[a]

System/subsystem	Mass, kg (lbm)	
Bioshield		139.4 (306.7)
Aeroshell		140.0 (308.0)
Aerodecelerator		169.2 (372.2)
Parachute and mortar		109.1 (240.0)
Lander:		872.3 (1919.1)
Structure	100.7 (221.5)	
Pyro	11.4 (25.1)	
Thermal control	90.9 (200.0)	
Power	83.8 (184.4)	
Telemetry	18.8 (41.4)	
Guidance and Control	58.8 (129.4)	
Communications	29.1 (64.0)	
Wire harness	25.7 (56.5)	
Science	70.0 (154.0)	
Contingency	94.7 (208.3)	
Explosive:		
Usable	196.3 (431.9)	
Residual	20.0 (44.0)	
Propulsion system inert	72.1 (158.6)	
Total estimated mass		1430.0 (3146.0)

[a] $\Delta V = 500\ m \cdot s^{-1}$; $I_s = 1961\ N \cdot s \cdot kg^{-1}$ (200 lbf • s/lbm).

Table 9. Launch vehicle performance summary

Item	Shuttle/Centaur
Launch date	12/89
Launch period, days	20
C_3, km^2/s^2	80
Required injected mass, kg	1430
Transit time, days	48
Deliverable mass, kg	4200
Transit time maximum mass, days	70

Table 10. Operational characteristics of typical explosive charge size propulsion units

Charge size, g	Average total thrust, N	Impulse reaction time,[a] μs	Average spacecraft acceleration, $m \cdot s^{-1}$(g)	Number of pulses/unit ($\gamma_f = 20\ s^{-1}$)[b]
2	400	105	0.30 (0.031)	19,247
3	600	91	0.45 (0.046)	12,831
5	1000	77	0.75 (0.076)	7,699
7	1400	69	1.05 (0.107)	5,499
10	2000	61	1.50 (0.153)	3,849
15	3000	53	2.25 (0.229)	2,566

[a]Estimate based on strong shock solution applicability.

[b]γ_f = firing rate, pulses per second.

Table 11. Preliminary cost assessment

Component	Nonrecurring costs, 10^6 dollars[a]	Recurring costs, 10^6 dollars[a,b]
Reservoir and delivery system	0.7	0.5
Laser	1.5	0.5
Plunger	5.0	1.0
Shock absorber	4.0	0.5
Muffler	0.7	0.3
Nozzle	4.0	1.0
Propellant	6.0	0.5
Contingency (30%)	6.6	1.3
Total	28.5	5.6

[a]Based on 1973 dollars.

[b]For production quantities of 3 to 5 units.

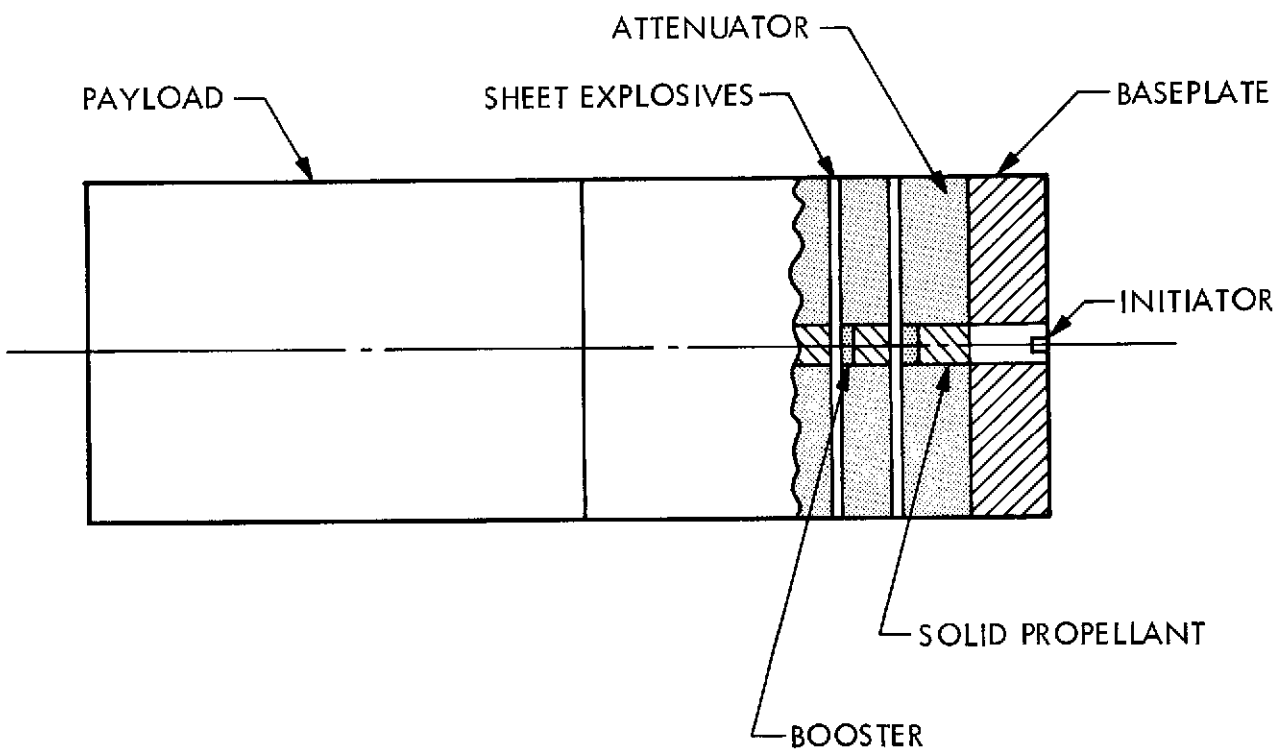

Fig. 1. Early conceptual design

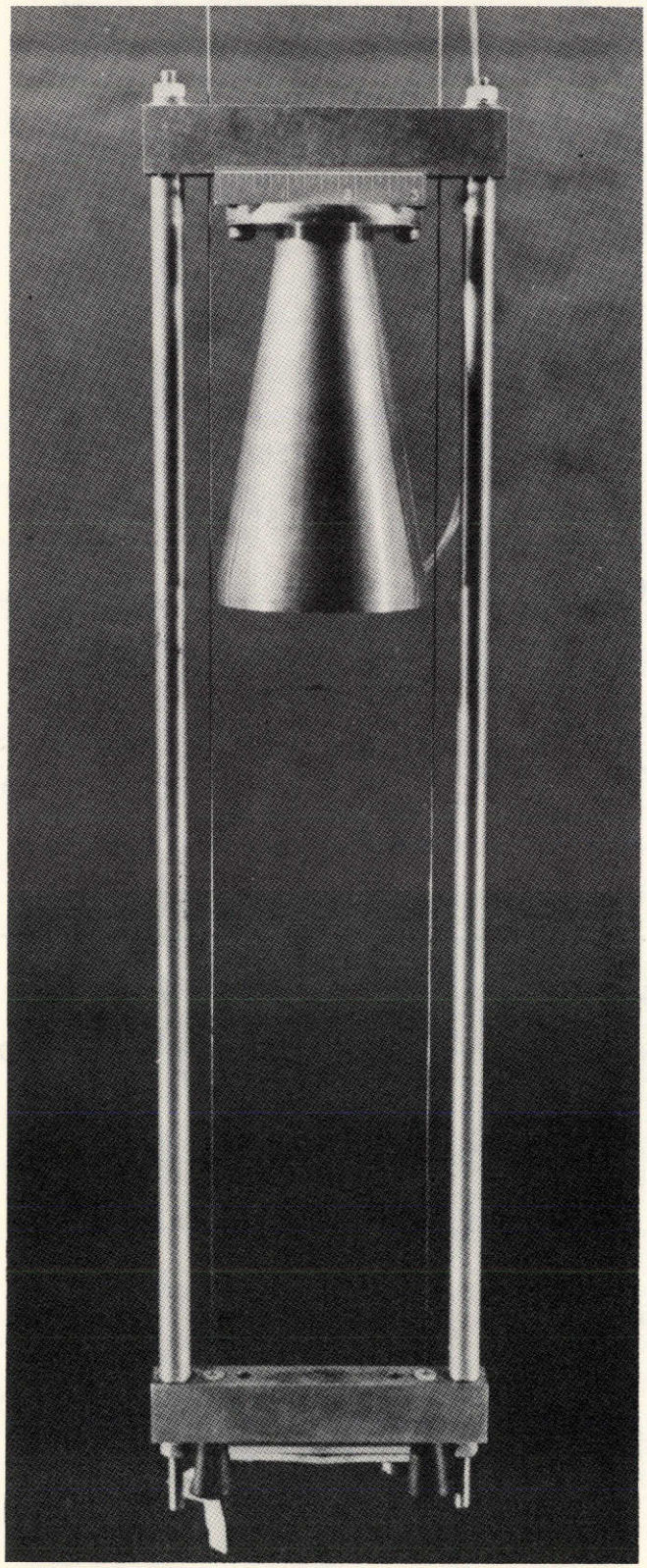

Fig. 2. Sled experiment test apparatus

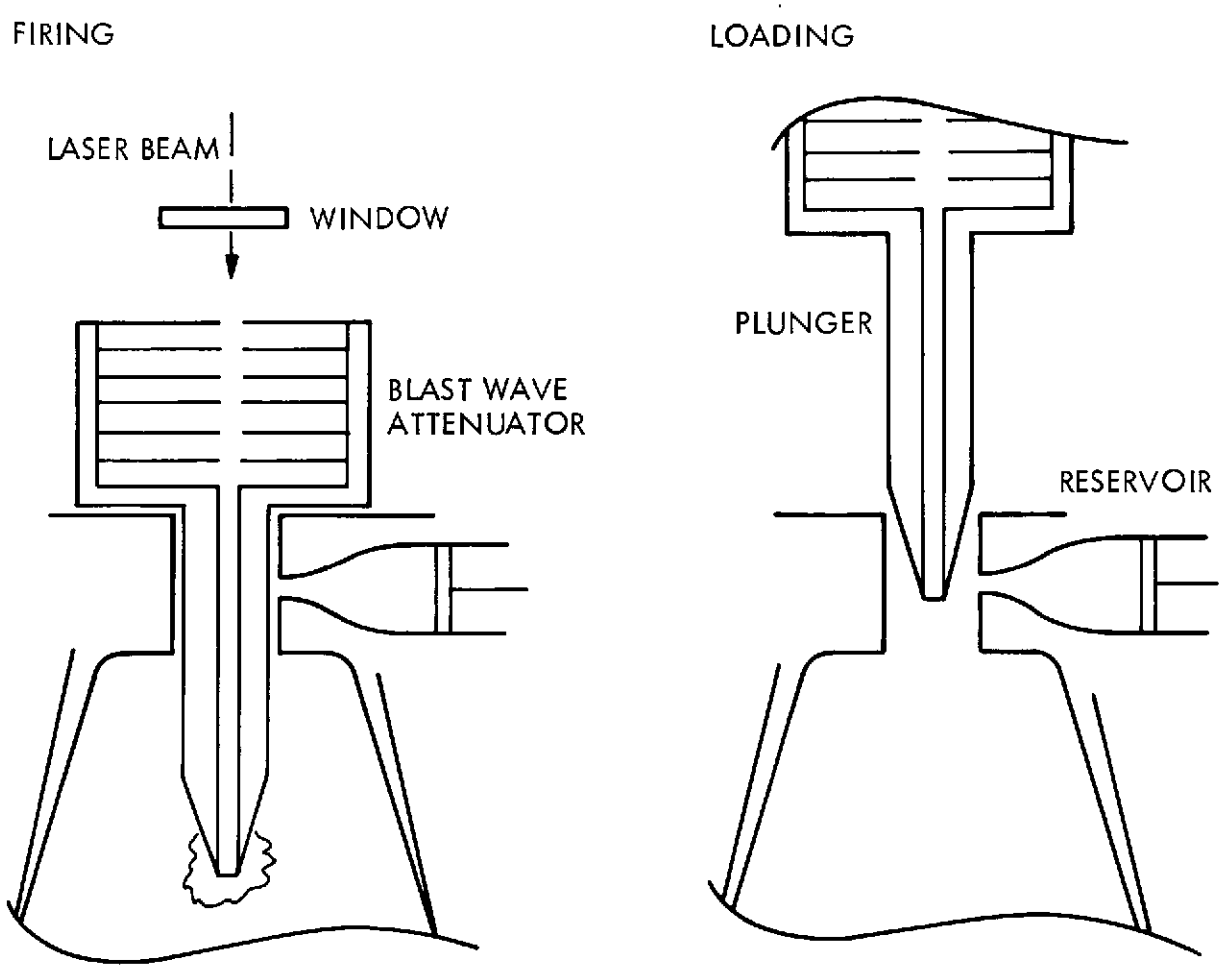

Fig. 3. Conceptual design mechanization

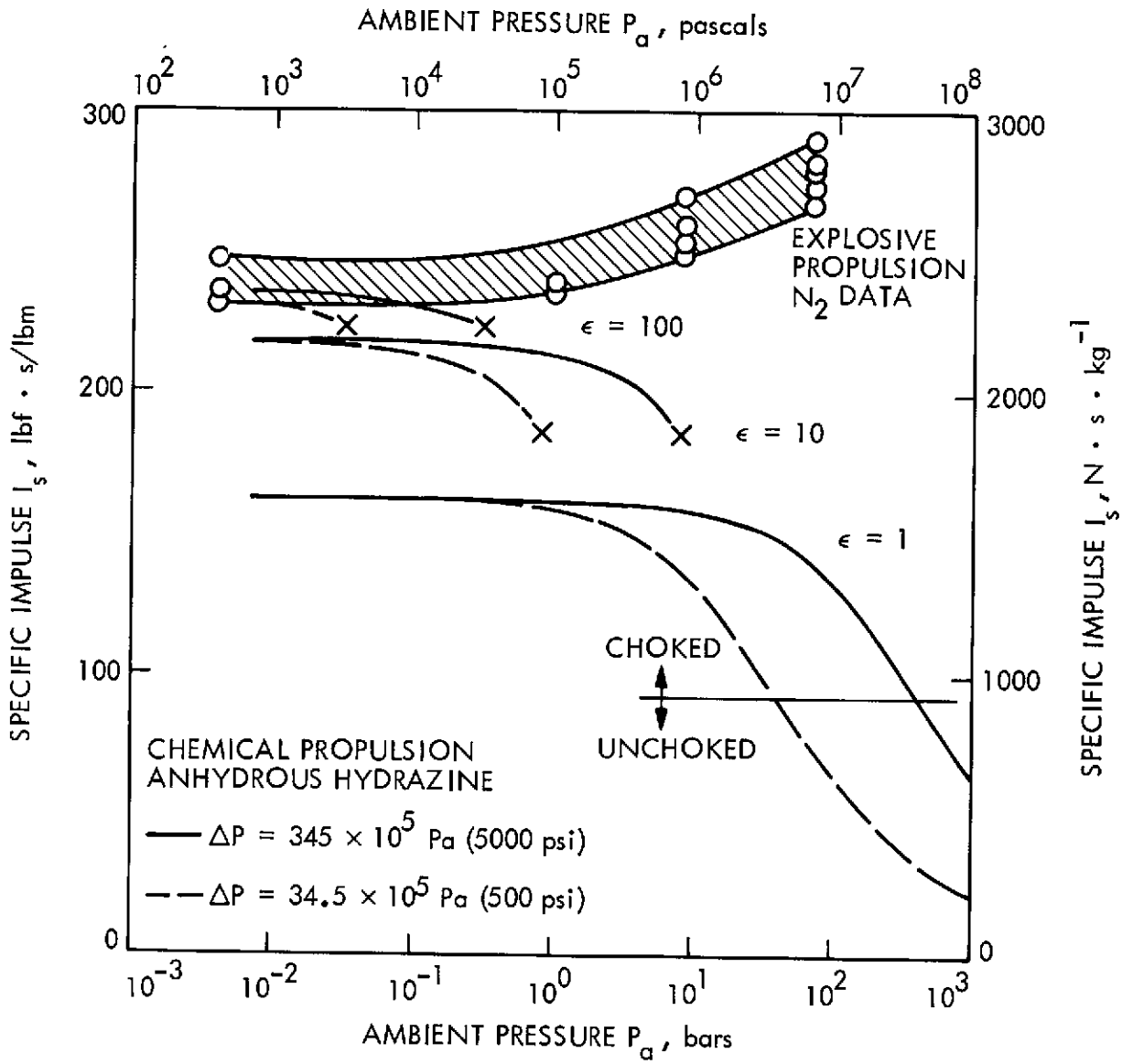

Fig. 4. Comparison of chemical and explosive propulsion performance

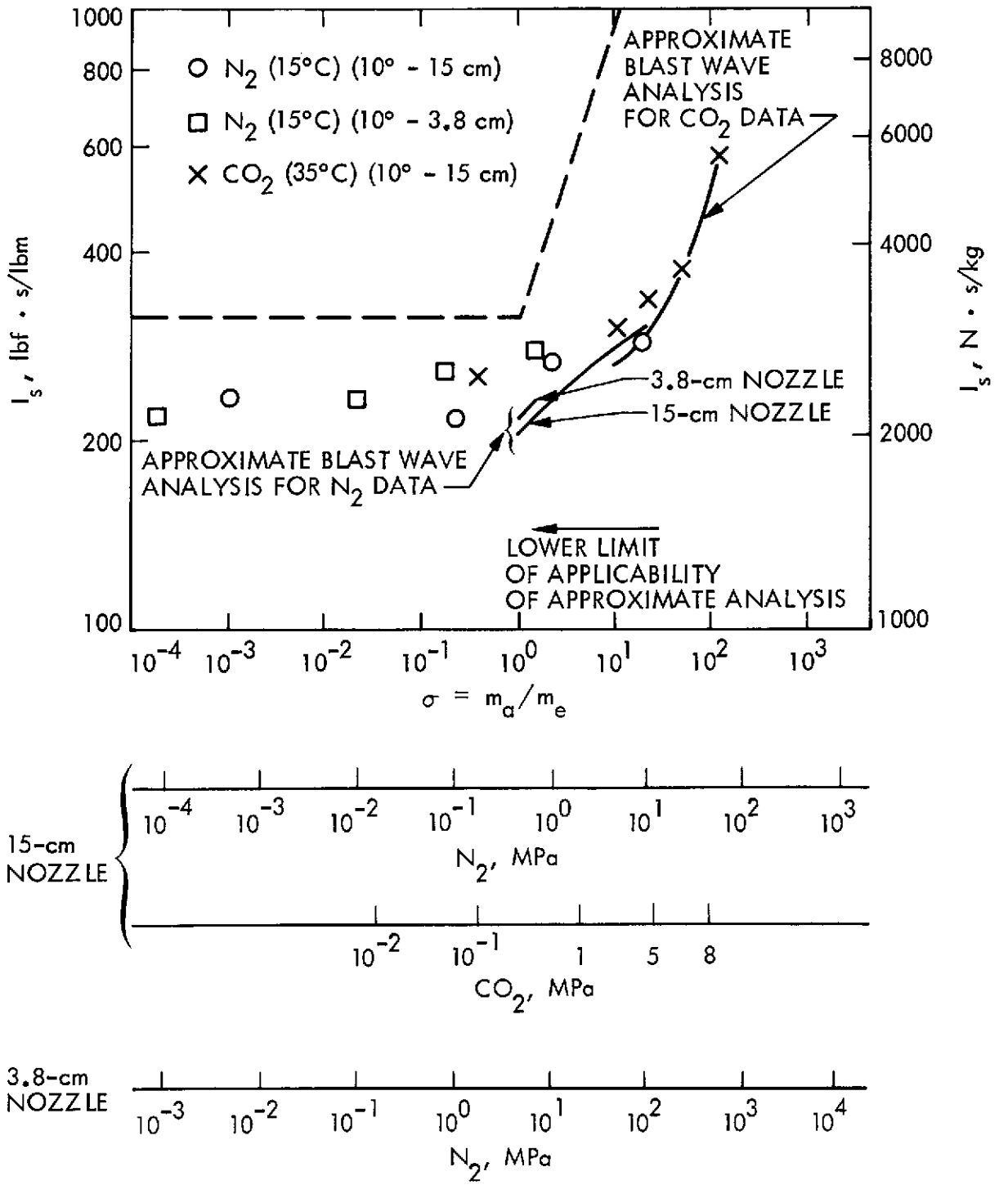

m_a = MASS OF ATMOSPHERIC GASES IN THE NOZZLE

m_e = MASS OF EXPLOSIVE CHARGE IN THE NOZZLE

Fig. 5. Experimental performance data for CO_2 and N_2 environments utilizing PETN explosives

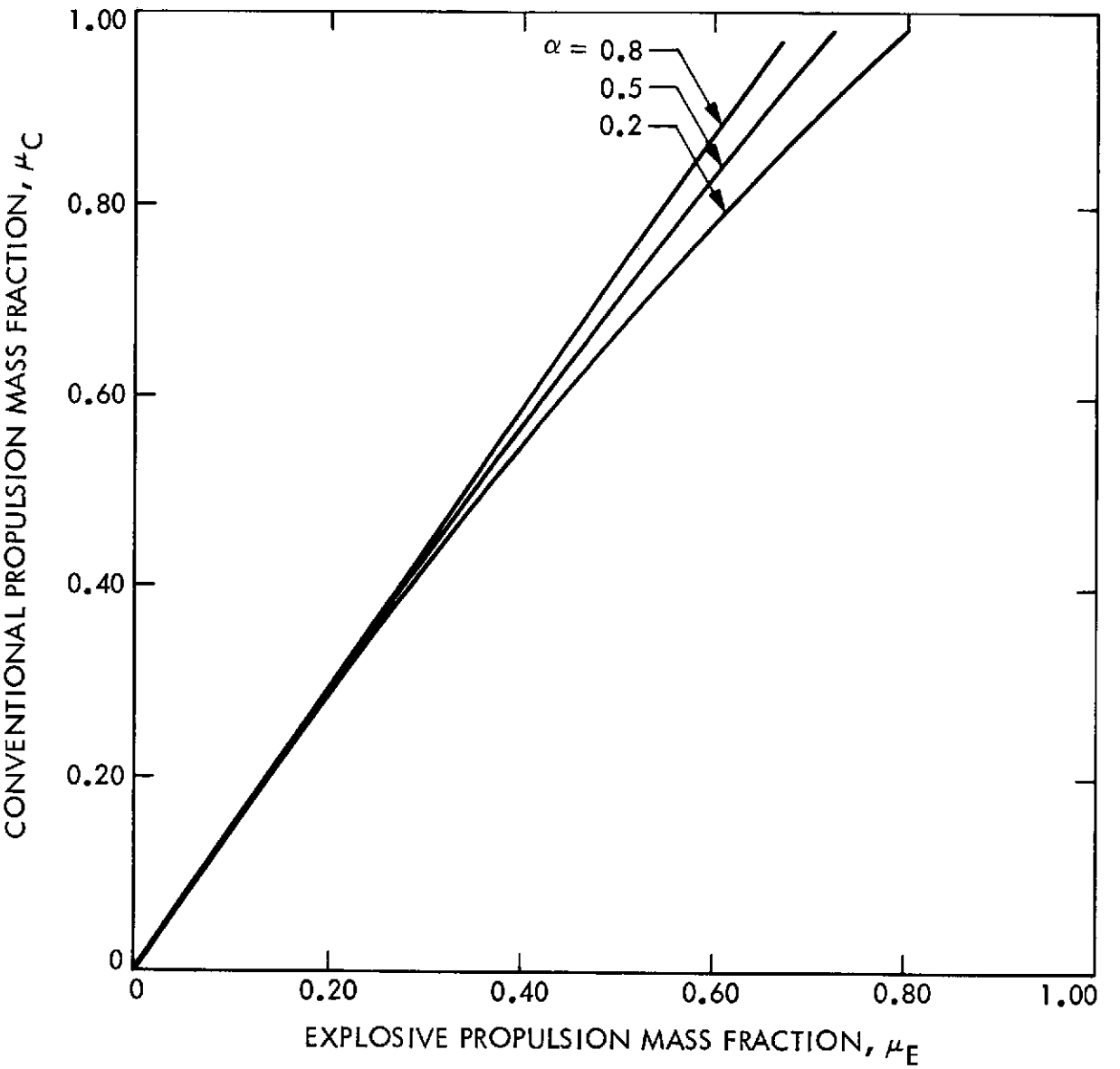

Fig. 6. Competitive comparison of propulsive mass fractions of conventional vs chemical explosive propulsion systems for $I_E/I_C = 1.5$

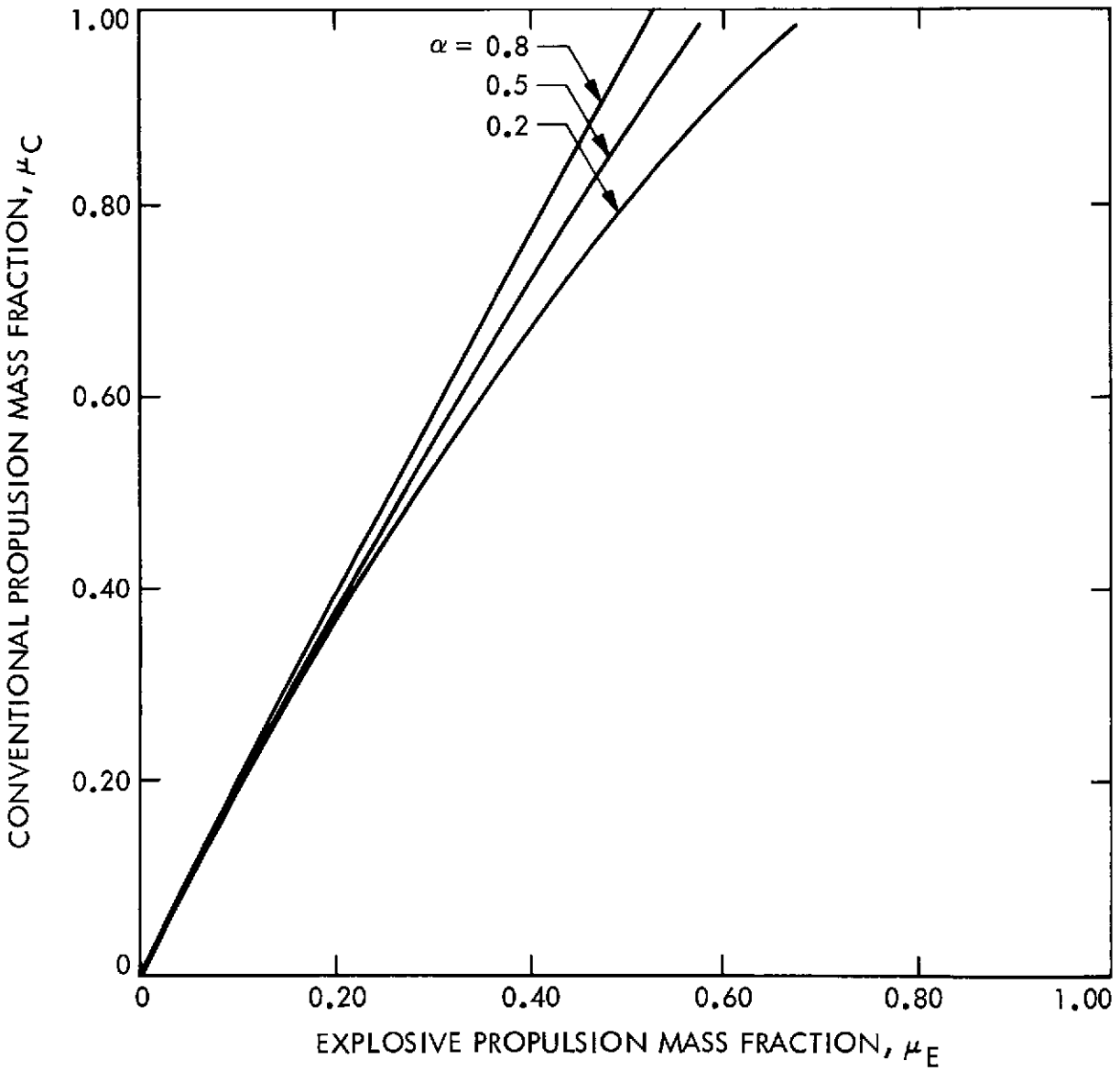

Fig. 7. Competitive comparison of propulsive mass fractions of conventional vs chemical explosive propulsion systems for $I_E/I_C = 2.0$

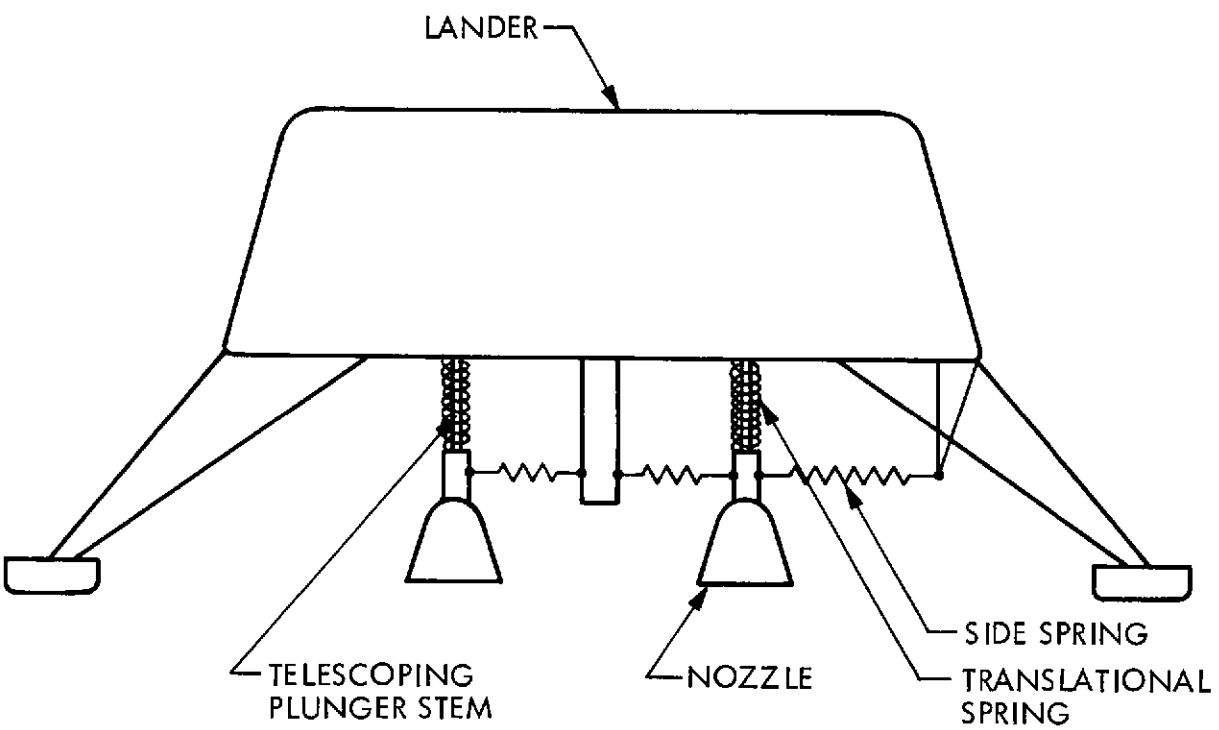

Fig. 8. Propulsion system integration

APPENDIX

PROPERTIES OF TYPICAL EXPLOSIVES
(Refs. 9 and 29)

Explosive	Composition, % (or formula)	Explosion temperature, K at 5 s	Normal density, g/cm^3	Detonation rate (P = normal), [a] m·s^{-1}	Detonation pressure, Pa×10^8(kbars)	Heat of explosion, J/g (cal/g)	Theoretical I_S N·s/kg (lbf·s/lbm)
Amatol, 80/20	Ammonium nitrate 80 TNT 20	Decomposes at 553	1.46	4500	74	2050 (490)	2030 (207)
Baratol	Barium nitrate 67 TNT 33	Ignites at 658	2.52	4500-5200	128-170		
Baronal	Barium nitrate 50 TNT 35 Aluminum 15	Ignites at 618	2.32	5450	172	4770 (1140)	3090 (315)
Butanetriol Trinitrate (BTTN) Liquid	$C_4H_7N_3O_9$	Decomposes at 503	1.52			6110 (1460)	3490 (356)
Composition A-3	RDX 91 Wax 9	Decomposes at 523	1.59	8100	260	5360 (1280)	3280 (334)
Composition B	RDX 60 TNT 40 Wax 1	Decomposes at 551	1.68	7840	258	5200 (1240)	3230 (329)
Composition C4	RDX 91 Plasticizer 9	563	1.59	8040	257	6360[a] (1520)	3570 (364)
Cyclonite (RDX)	$C_3H_6N_6O_6$	Decomposes at 533	1.65	8180	276	5360 (1280)	3280 (334)
Cyclotol 75/25	RDX 75 TNT 25		1.71	7940	270	5150 (1230)	3210 (327)
Cyclotol 70/30	RDX 70 TNT 30	Decomposes at 538	1.73	8060	281	5070 (1210)	3190 (325)
Cyclotol, 65/35	RDX 65 TNT 35	Decomposes at 543	1.72	7980	274	5070 (1210)	3180 (324)
Cyclotol, 60/40	RDX 60 TNT 40	Decomposes at 553	1.72	7900	269	5020 (1200)	3170 (323)
Cyclotrimethylene Trinitrosamine	$C_3H_6N_6O_3$	493	1.42	7000-7300	174-189	3670 (876)	2710 (276)

Explosive	Composition, % (or formula)		Explosion temperature, K at 5 s	Normal density, g/cm^3	Detonation rate (P = normal), [a] m·s^{-1}	Detonation pressure, Pa×10^8(kbars)	Heat of explosion, J/g (cal/g)	Theoretical I_s N·s/kg (lbf·s/lbm)	
DBX	Ammonium nitrate RDX TNT Aluminum	21 21 40 18	Ignites at 673	1.65	6600	179	7120 (1700)	3780	(385)
DATNB	$C_6H_5N_5O_6$			1.65	7500	232	12100 (2880)	4910	(501)
DDNP	$C_6H_2N_4O_5$		468	1.5	6600	163	3430 (820)	2620	(267)
DEGN liquid	$C_4H_8N_2O_7$		510	1.38	6760	158	3520 (841)	2660	(271)
Bis Fumarate (DNPF)	$C_{10}H_{12}N_4O_{12}$		Smokes at 523	1.49	6050	137	3210 (767)	2540	(259)
Dynamite (LVD)	99.5/0.5RDX/ 1-MA TNT Tripentacry-thritol 68/32 Vistac No1/DOS Cellulose acetate, LH-1	17.5 67.8 8.6 4.1 2.0	Ignites at 753	0.9	4400	43.5	2620 (625)	2290	(233)
Dynamite (MVD)	RDX TNT Starch SAE No. 10 Oil Vistanex oil gel	75 15 5 4 1		1.1	6000-6600	99-120	3910 (935)	2810	(286)
Explosive D	$C_6H_6N_4O_7$		Decomposes at 591	1.55	6850	181	3350 (800)	2590	(264)
H-6	RDX TNT Aluminum D-2 wax Calcium Chloride	45 30 20 5 0.5	883	1.71	7190	221	3860 (923)	2790	(284)

Explosive	Composition, % (or formula)		Explosion temperature, K at 5 s	Normal density, g/cm^3	Detonation rate (P = normal), a m•s^{-1}	Detonation pressure, Pa × 10^8(kbars)	Heat of explosion, J/g (cal/g)	Theoretical I_s N•s/kg (lbf•s/lbm)	
Haleite (EDNA)	$C_2H_6N_4O_4$		Decomposes at 462	1.49	7570	214	5360 (1280)	3280	(334)
HBX-1	RDX TNT Aluminum D-2 wax Calcium chloride	40 38 17 5 0.5	753	1.69	7220	221	3850 (919)	2780	(283)
HBX-3	RDX TNT Aluminum D-2 wax Calcium chloride	31 29 35 5 0.5	773	1.81	6920	217	3670 (877)	2720	(277)
HEX-4	Potassium perchlorate Aluminum, atomized RDX Asphaltum	32 48 16 4	793	1.37			7790 (1860)	3950	(403)
HEX-48	Potassium perchlorate Aluminum, flaked RDX Asphaltum	32 48 16 4	818	0.69			7290 (1740)	3820	(389)
Beta HMX	$C_4H_8N_8O_8$		600	1.84	9120	383	5690 (1360)	3370	(344)
HTA-3	HMX TNT Aluminum	49 29 22	Flames erratically at 643	1.90	7870	294	4950 (1190)	3160	(322)
Lead Azide	PbN_6		Explodes at 613	4.0	5180	269	1540 (367)	1760	(179)
Lead Styphnate	$PbC_6H_3N_3O_9$		Explodes at 555	2.9	5200	196	1910 (457)	1961	(200)

Explosive	Composition, % (or formula)	Explosion temperature, K at 5 s	Normal density, g/cm^3	Detonation rate (P = normal), [a] m·s^{-1}	Detonation pressure, Pa × 10^8 (kbars)	Heat of explosion, J/g (cal/g)	Theoretical I_s N·s/kg (lbf·s/lbm)
Nitromannite	$C_6H_8N_6O_{18}$	448	1.73	8260	295	5820-6360 (1390-1520)	3410 (348-364)
Mercury Fulminate	$HgC_2N_2O_2$	Explodes at 483	4.0	5000	250	1790 (427)	1890 (193)
Minol-2	Ammonium nitrate 40 TNT 40 Aluminum 20	Ignites at 708	1.68	5820	142	6780 (1620)	3690 (376)
MOX-1	Ammonium perchlorate 35.0 Aluminum, atomized 26.2 Magnesium, atomized 26.2 Tetryl 9.7 Calcium stearate 1.9 Graphite, artificial 1.0	558	2.0			8710 (2080)	4180 (426)
MOX-2B	Ammonium perchlorate 35.0 Aluminum, atomized 52.4 5.8%RDX & 3.9%TNT coated or ammonium perchlorate 9.7 Calcium stearate 1.9 Graphite, artificial 1.0	648	2.03	4830	119	6150 (1470)	3510 (358)

Explosive	Composition, % (or formula)		Explosion temperature, K at 5 s	Normal density, g/cm^3	Detonation rate (P = a normal), $m \cdot s^{-1}$	Detonation pressure, Pa × 10^8(kbars)	Heat of explosion, J/g (cal/g)	Theoretical I_s N•s/kg (lbf•s/lbm)	
MOX-3B	Potassium nitrate	18	813	2.0			4100 (980)	2860	(292)
	Aluminum	50							
	29.1%RDX, 0.9% Wax, 2% TNT	32							
	Calcium stearate	2							
	Graphite, artificial	1							
MOX-4B	Barium nitrate	18	883	2.0			2970 (709)	2440	(249)
	Aluminum, atomized	50							
	29.1% RDX, 0.9% wax, 2% TNT	32							
	Calcium stearate	2							
	Graphite, artificial	1							
MOX-6B	Aluminum, atomized	49.2	783	2.0			3140 (750)	2510	(256)
	Cupric oxide	19.7							
	28.7% RDX coated, 0.9% wax	29.6							
	Graphite, artificial	1.5							
Nitroguanidine	$CH_4N_4O_2$		Decomposes at 548	1.55	7650	227	3020 (721)	2460	(251)
Octol, 70/30	HMX	70	Flames erratically at 608	1.80	8380	316	4480 (1070)	3000	(306)
	TNT	30							
Octol, 75/25	HMX	75	Flames erratically at 623	1.81	8640	338	4730 (1130)	3080	(314)
	TNT	25							
PB-RDX	RDX	90	Smokes at 548	1.68	8230	285	4120 (983)	2870	(293)
	Polystyrene (unmodified)	8.5							
	Dioctylphthalate	1.5							

Explosive	Composition, % (or formula)		Explosion temperature, K at 5 s	Normal density, g/cm^3	Detonation rate (P = normal), a $m \cdot s^{-1}$	Detonation pressure, Pa $\times 10^8$(kbars)	Heat of explosion, J/g (cal/g)	Theoretical I_s N·s/kg (lbf·s/lbm)	
Pentolite, 50/50	PETN TNT	50 50	Decomposes at 493	1.66	7470	231	5110 (1220)	3200	(326)
PETN	$C_5H_8N_4O_{12}$		Decomposes at 498	1.70	8300	293	5820 (1390)	3410	(348)
Picratol, 52/48	Explosive D TNT	52 48	Decomposes at 558	1.63	6970	198			
Picric acid	$C_6H_3N_3O_7$		Decomposes at 593	1.71	7350	231	4190 (1000)	2890	(295)
Tetryl	$C_7H_5N_5O_8$		Ignites at 530	1.71	7850	263	4520-4730 (1080-1130)	3010-3880	(307-314)
Tetrytol, 70/30	Tetryl TNT	70 30	Ignites at 593	1.60	7340	216			
TNT	$C_7H_5N_3O_6$		Decomposes at 748	1.56	6830	181	4520 (1080)	3010	(307)
Torpex	RDX TNT Aluminum	42 40 18	Decomposes at 533	1.81	7500	254	7540 (1800)	3880	(396)
TPEON	$C_{15}H_{24}N_8O_{26}$		498	1.56	7650	228	4560 (1090)	3020	(308)
Tritonal, 80/20	TNT Aluminum	80 20	Decomposes at 743	1.72	6700	194	7410 (1770)	3850	(393)
Veltex	HMX Nitrocellulose (13.15% N) Nitroglycerin 2-nitrodiphenyl-amine Triacetin	70 15 10.7 1.3 3		1.72	8500	311	5150 (1230)	3210	(327)

[a]Calculated.

NASA – JPL – Coml., L.A., Calif.